Biochemical and Biophysical Research Communications 432 (2013) 378–383

Contents lists available at SciVerse ScienceDirect

Biochemical and Biophysical Research Communications

journal homepage: www.elsevier.com/locate/ybbrc

α-Lipoic acid attenuates coxsackievirus B3-induced ectopic calcification in heart, pancreas, and lung

Hyo Shin Kim [a,d,e], Hong-In Shin [b], Hyun-Sook Lim [c], Tae Yoon Lee [d], Kyunghee Lee [d,e,*], Daewon Jeong [d,e,*]

[a] Department of Clinical Pathology, Taekyeung College, Gyeungsan 712-719, Republic of Korea
[b] IHBR, Department of Oral Pathology, School of Dentistry, Kyungpook National University, Daegu 700-412, Republic of Korea
[c] Department of Public Health Administration, Hanyang Women's University, Seoul 133-793, Republic of Korea
[d] Department of Microbiology, Yeungnam University College of Medicine, Daegu 705-717, Republic of Korea
[e] Aging-Associated Vascular Disease Research Center, Yeungnam University College of Medicine, Daegu 705-717, Republic of Korea

ARTICLE INFO

Article history:
Received 11 January 2013
Available online 26 January 2013

Keywords:
Coxsackievirus B3
Ectopic calcification
Osteogenic signal
α-Lipoic acid

ABSTRACT

Ectopic mineralization of soft tissues is known to be a typical response to systemic imbalance of various metabolic factors as well as tissue injury, leading to severe clinical consequences. In this study, coxsackievirus B3 (CVB3) infection in mice resulted in significant tissue injury, especially in the heart and pancreas. Inflammatory damage and apoptotic cell death were observed in CVB3-infected heart and pancreas tissues. Along with tissue damage, substantial ectopic calcification was detected in CVB3-infected heart, pancreas, and lung tissues, as determined by von Kossa staining and calcium content quantification. In addition, CVB3 infection induced upregulation of osteogenic signals, including six genes (*BMP2*, *SPARC*, *Runx2*, osteopontin, collagen type I, and osterix) in the heart, three genes (*SPARC*, osteopontin, and collagen type I) in the pancreas, and two genes (*BMP2* and alkaline phosphatase) in the lung, as determined by quantitative real-time PCR analysis. Intriguingly, we showed that α-lipoic acid diminished CVB3-mediated inflammatory and apoptotic tissue damage, subsequently ameliorating ectopic calcification via the suppression of osteogenic signals. Collectively, our data provide evidence that ectopic calcification induced by CVB3 infection is implicated in the induction of osteogenic propensity, and α-lipoic acid may be a potential therapeutic agent to ameliorate pathologic calcification.

1. Introduction

Pathological ectopic mineralization has been reported to be responsible for serious clinical outcomes in humans [1]. Soft tissues such as the heart, kidney, stomach, lung, articular cartilage, and blood vessels are known to be susceptible to ectopic calcification [1,2]. Pathophysiological conditions that predispose soft tissues to abnormal calcification include microbial or viral infection, inflammation, metastatic cancer, aging, chronic kidney disease, diabetes, dyslipidemia, oxidant insults, hypercalcemia, and hyperphosphatemia [3–5]. Clinical classification of ectopic calcification generally encompasses both dystrophic and metastatic calcification. Dystrophic calcification is superimposed onto damaged tissues as a result of infection, necrotic cell death, and inflammation. For example, dystrophic calcification has been observed in tuberculosis lesions caused by pulmonary mycobacterial infection as well as in old infarcts [6]. Metastatic calcification is a cell-mediated, highly regulated process that represents calcium deposition onto undamaged tissues as a result of mineral imbalances in the circulating blood, leading to systemic extracellular matrix mineralization [5].

Final destined cells, considered to be terminal cells in specific tissues, can transdifferentiate into unwanted cells with entirely different properties distinct from intact cells. For instance, osteogenic transdifferentiation of cells within soft tissues results in localized and systemic calcification as well as irreversible dysfunction at the cellular and tissue levels. One of the most well known models of cell-mediated ectopic calcification is transdifferentiation of vascular smooth muscle cells into osteoblast-like cells, showing the formation of apoptotic bodies and membrane-bound matrix vesicles as well as the induction of osteogenic genes, including *BMP2*, *Runx2*, osterix, collagen type I, alkaline phosphatase, osteopontin, and osteocalcin [7–9]. To explore vascular calcification, murine knockout models of various genes encoding fibroblast growth factor 23, Klotho, matrix Gla protein, osteoprotegerin, fetuin A, apolipoprotein E, and low-density lipoprotein receptor as well as a nephrectomy model and stimulants, including vitamin D, nicotin, and warfarin, have been reported [10–13].

Despite these efforts, previous experimental animal models are not suitable for studying the pathological calcification process, and

* Corresponding authors. Address: Department of Microbiology, Yeungnam University College of Medicine, 317-1 Daemyung-Dong, Nam-Gu, Daegu 705-717, Republic of Korea. Fax: +82 53 653 6628.
E-mail addresses: kyungheelee@ynu.ac.kr (K. Lee), dwjeong@ynu.ac.kr (D. Jeong).

0006-291X/$ - see front matter © 2013 Elsevier Inc. All rights reserved.
http://dx.doi.org/10.1016/j.bbrc.2013.01.061

it remains difficult to analyze the mechanism of ectopic calcification in other soft tissues except for aortic blood vessels. Our recent study reported that mice infected with coxsackievirus B3 (CVB3), human pathogenic picornavirus with a single-stranded RNA genome, show increased serum levels of inflammatory cytokines, including IL-1β, TNF-α, and the receptor activator of NF-κB ligand (RANKL), leading to substantial ectopic calcification in the heart, pancreas, and lung [14]. This model possesses time- and cost-saving advantages and can efficiently induce soft tissue calcification *in vivo*. Further, it was proven at the cellular level that RANKL is linked to *in vitro* cardiac fibroblast calcification by inorganic phosphate via induction of osteogenic signals, including *BMP2*, *SPARC*, *Runx2*, Fra-1, and NF-κB. In this study, we tried to analyze the multiple causative factors of ectopic calcification at the tissue level. We observed that CVB3-infected mice exhibited inflammatory and apoptotic tissue damage as well as osteogenic gene induction, specifically in the heart, pancreas, and lung. We further evaluated α-lipoic acid (1,2-dithiolane-3-pentanoic acid, ALA) as a potential therapeutic target for the prevention of ectopic calcification.

2. Materials and methods

2.1. Virus and mice

CVB3 (Nancy strain) was prepared in cultures of HeLa cells grown in DMEM (HyClone, Logan, UT, USA) supplemented with 10% FBS (HyClone) and antibiotics (Invitrogen, Carlsbad, CA, USA). Virus titer was measured in PFU/ml by plaque assay. Seven-week-old BALB/c mice were purchased from Central Lab Animal (Seoul, Korea) and maintained at the animal facility of Yeungnam University College of Medicine. All animal experiments were approved by the institutional review board of Yeungnam University Medical Center and were in compliance with the Guide for the Care and Use of Laboratory Animals.

2.2. Study design

Male mice at 7 weeks of age were injected intraperitoneally (i.p.) with CVB3 (2×10^4 PFU) in PBS or with PBS alone (control). ALA (10 mg/kg, Bukwang Pharm Corp., Seoul, Korea) was pre-injected 1 day before CVB3 injection. Then, ALA was injected the same time as virus administration as well as every other day thereafter. Mice were sacrificed on day 14 or at the indicated times after CVB3 infection for collection of soft tissues.

2.3. Histological analysis

Specimens fixed with 3.7% formaldehyde were embedded in paraffin and sectioned at a thickness of 4 μm. Paraffin-embedded sections of soft tissues were deparaffinized and subjected to hematoxylin and eosin (HE) staining for histological analysis or von Kossa staining for analysis of calcium deposition. Images were scanned with an Aperio ScanScope Model T3 and were analyzed with ImageScope software (Aperio Technologies, Vista, CA, USA).

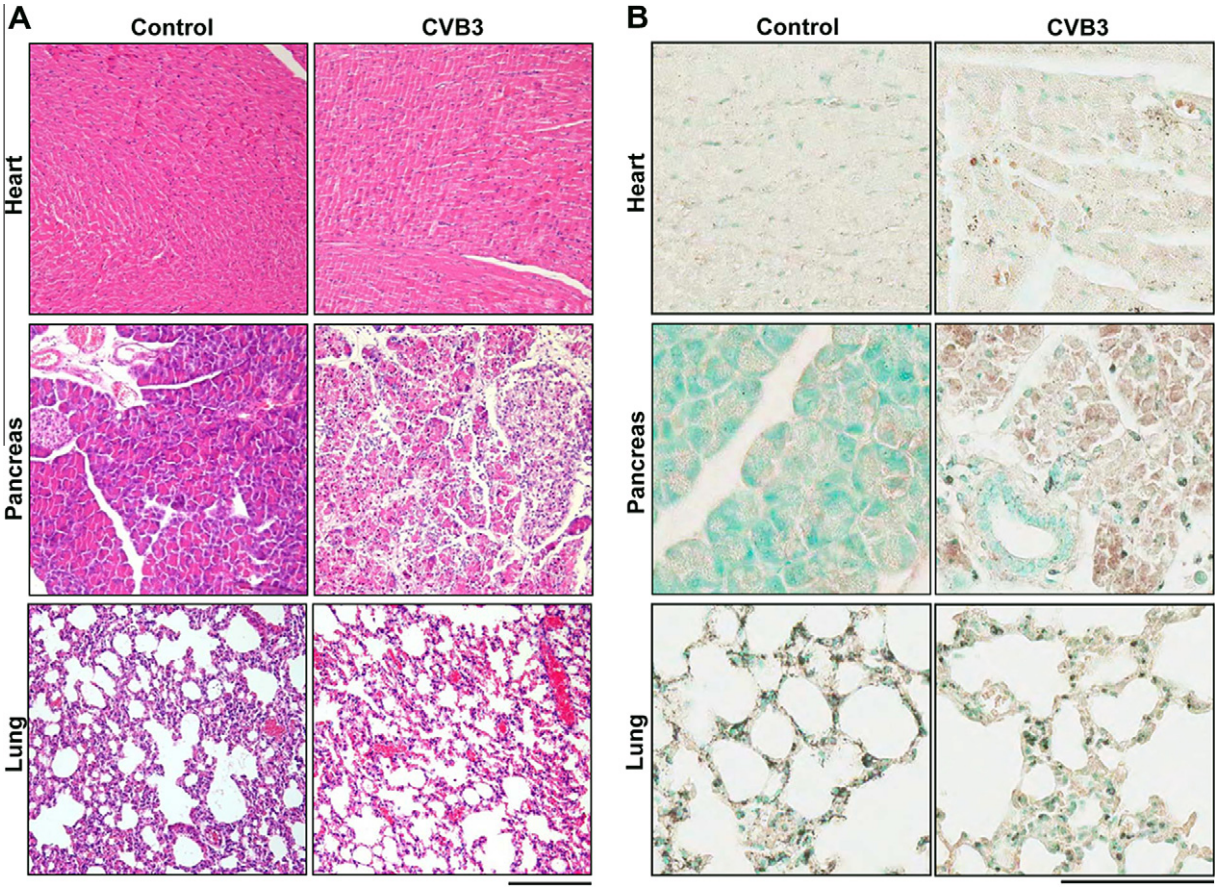

Fig. 1. Histological analysis and TUNEL assay of tissues from CVB3-infected mice. (A) Tissue sections from control ($n = 7$) and virus-infected ($n = 7$) mice were stained with HE at 3 days after CVB3 infection. Representative images are shown. Scale bar, 100 μm. (B) Assessment of apoptosis in heart, pancreas, and lung tissues from control ($n = 7$) and CVB3-infected mice ($n = 7$) at 14 days post-injection. Abundant brown staining of CVB3-infected heart and pancreas is shown. Representative images are shown. Scale bar, 100 μm.

2.4. Calcium quantification

For quantification of calcium in the heart, pancreas, and lung tissues were semi-dried and weighed. The tissues were then chopped into small pieces, and calcium deposited in tissues was extracted with 0.6 N HCl. After rocking vigorously at 4 °C for 48 h, the suspension was centrifuged at 10,000×*g* for 10 min at 4 °C. Calcium content of the resulting supernatant was determined colorimetrically using a QuantiChrome Calcium Assay Kit (BioAssay Systems, Hayward, CA, USA) and was normalized according to tissue weight.

2.5. Apoptosis assay

Apoptotic cells in heart, pancreas, and lung tissues from CVB3-infected or control mice were detected by using a TACS 2 TdT DAB *in situ* apoptosis detection kit (Trevigen, Gaithersburg, MD, USA) according to the manufacturer's instructions. Briefly, paraffin-embedded sections were deparaffinized by heating at 57 °C for 20 min and rehydrated by sequential washing in xylene as well as 100%, 95%, and 70% ethanol prior to the labeling reaction. Following protease K digestion and quenching of endogenous peroxidase with 2% hydrogen peroxide (H_2O_2) solution, tissue sections were covered with deoxynucleotidyl transferase (TdT), TdT dNTP mix, and Co^{2+} cations in TdT buffer and incubated in a humidified chamber at 37 °C for 60 min. Labeled cells were detected by the conversion of diaminobenzidine by streptavidin-horseradish peroxidase. The slides were counterstained with 1% methyl green for 3 min. All images of the samples were taken using an Aperio ScanScope Model T3 (Aperio Technologies).

2.6. Quantitative real-time PCR

Total RNA was extracted from tissues using TRIZOL reagent (Invitrogen). Two micrograms of total RNA was reverse-transcribed into cDNA using a M-MLV reverse transcription kit (Invitrogen). Quantitative real-time RT-PCR was performed using SYBR Premix Ex Taq (Takara Bio Inc, Japan) on the Applied Biosystems 7500 Sequence Detection System and software (Applied Biosystems, Carlsbad, CA, USA). Relative gene expression levels were determined by the comparative ΔCt method, and target gene *Ct*-values were standardized against *β-actin* expression. Primers used were bone morphogenetic protein 2 (*BMP2*), 5′-TTTGCACCAAGATGAACACAGC-3′ and 5′-GCTTCCGCTGTTTGTGTTTG-3′; *SPARC*, 5′-CTGCGTGTGAAGAAGATCCA-3′ and 5′-TGGGACAGGTACCCATCAAT-3′; *Runx2*, 5′-AGATGATGACACTGCCACCTCTG-3′ and 5′-GCTCTCAGTGAGGGATGAAATGC-3′; alkaline phosphatase (*Alp*), 5′-AACACCAACGCTCAGGTCCC-3′ and 5′-CTGAGTGGTGTTGCATCGCGT-3′; osteocalcin (*OCN*), 5′-CTAGCAGACACCATGAGGACC-3′ and 5′-TGCCCTCCTGCTTGGACATGAA-3′; osteopontin (*OPN*), 5′-CCCATCTCAGAAGCAGAATCT-3′ and 5′-TTGCTTGGAAGAGTTTCTTGCT-3′; bone sialoprotein (*IBSP*), 5′-TTTCCAGTCCAGGGAGGCAG-3′ and 5′-TCCGCCTCCTGGTCTTCATTC-3′; collagen, type I, alpha 1 (*Col1α1*), 5′-TGGTGCTAAGGGTGAAGCTG-3′ and 5′-GCAATACCAGGAGCACCATTG-3′; osterix (*Osx*), 5′-CTCTCTGCTTGAGGAAGAAG-3′ and 5′-TATGGCTTCTTTGTGCCTCCTTT-3′; *β-actin*, 5′-CCCTGAAGTACCCCATTGAA-3′ and 5′-CTTTTCACGGTTGGCCTTAG-3′.

2.7. Statistical analysis

All results are expressed as means ± SD of at least three independent experiments or the indicated number of mice. Multiple

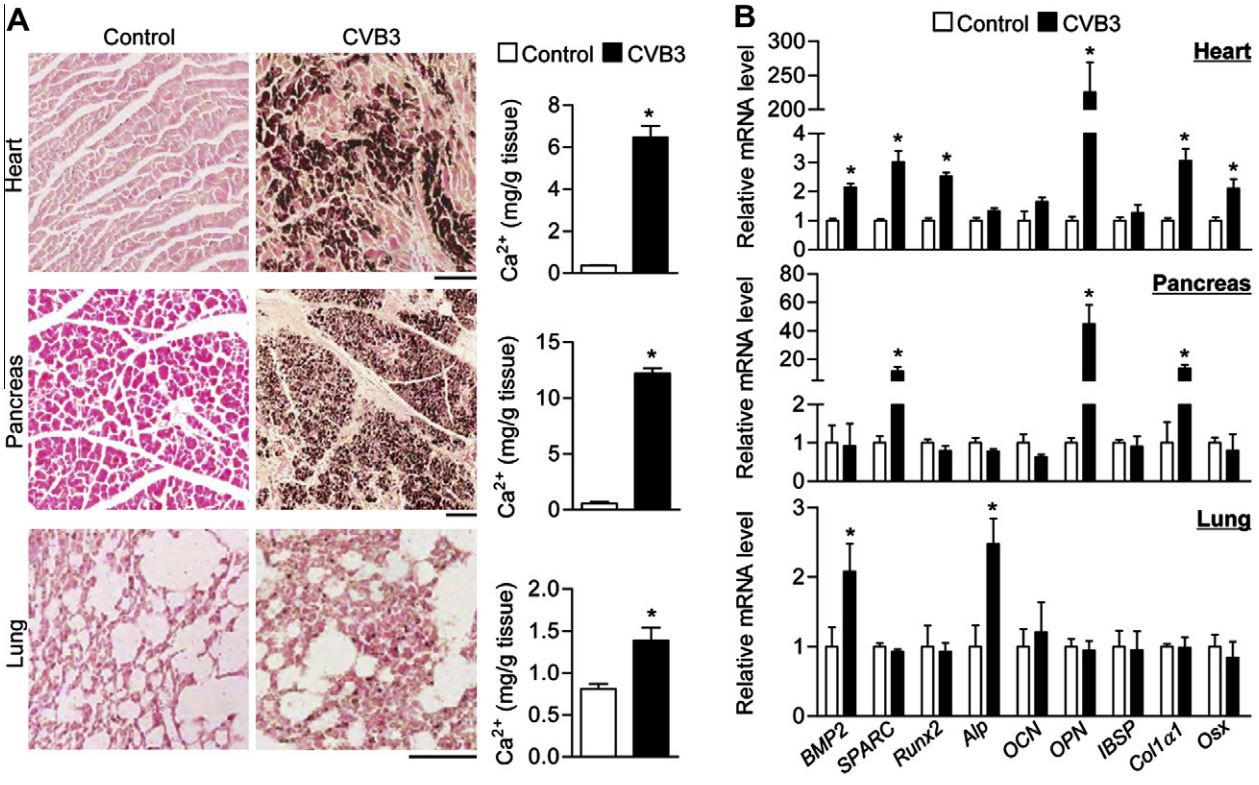

Fig. 2. Ectopic calcification and activation of osteogenic signals induced by CVB3 infection. (A) Heart, pancreas, and lung tissues from control ($n = 5$) and virus-infected ($n = 8$) mice were stained with von Kossa and calcium content was quantified. Representative images are shown. Scale bars, 100 μm. Quantitative data are presented as milligrams of calcium per gram of tissue as well as means ± SD. $^*P < 0.01$. (B) Tissue expression levels of osteogenic marker genes, including bone morphogenetic protein 2 (*BMP2*), *SPARC*, *Runx2*, alkaline phosphatase (*Alp*), osteocalcin (*OCN*), osteopontin (*OPN*), bone sialoprotein (*IBSP*), collagen, type I, alpha 1 (*Col1α1*), and osterix (*Osx*), in control ($n = 5$) and virus-infected ($n = 5$) mice were determined by quantitative real-time PCR. Quantification of mRNA expression ($2^{-\Delta\Delta}Ct$ method) is represented as a fold difference relative to control and is normalized to an endogenous control (*β-actin*). Values are expressed as means ± SD. $^*P < 0.01$.

comparison between three or more groups was performed by analysis of variance (ANOVA) using the SPSS 18.0 software package. When significant differences were found, pairwise comparisons between each group were carried out using two-tailed Student's *t* test. A *P* value of <0.05 was considered to be significant.

3. Results

3.1. Tissue damage caused by CVB3 infection

We extensively examined pathological signs in BALB/c mice following CVB3 infection. At three to four days after infection, mice exhibited reduced exercise performance as well as decreased food intake compared with control mice. A large amount of undigested food also remained in the intestinal tract of infected mice at 7 days post-infection. At 14 days post-infection, the survival rate of CVB3-infected mice had decreased by 26%, and the average weight of surviving mice was reduced by 23% compared with control animals. As shown in Fig. 1(A), intensive analysis of CVB3-infected mice was conducted at the tissue and cellular levels at three days post-infection. Cardiac myocytes showed altered nuclear morphology with irregular size and shape, and the arrangement of cells was not regular. In pancreatic acinar cells and islets of Langerhans from CVB3-infected mice, nuclear aberrations such as nuclear cleft and condensed chromatin were accompanied by cytoplasmic abnormalities. Further, intense inflammatory cell infiltration was observed in interstitial cells in the pancreas. At 14 days post-infection, inflammatory cells, including lymphocytes, were still apparent in the heart and pancreas (Supplementary Fig. 1), indicating CVB3-mediated inflammatory damage in virus-infected tissues. We also observed reduced thickness of subcutaneous fat tissue without any other apparent damage, whereas there were no phenotypic changes in other tissues, including the spleen, kidney, brain, liver, aorta, skeletal muscle, fat, and testis (Supplementary Fig. 1). To analyze apoptotic tissue damage, TUNEL assay was performed on CVB3-infected tissues. TUNEL assay-positive cells were easily detectable in pancreas and heart tissues (Fig. 1B). Apoptotic cell numbers apparently increased in pancreatic acinar cells, whereas relatively low numbers of apoptotic cells were detected in duct-lining pancreatic cells.

3.2. Ectopic calcification and osteogenic signal stimulation induced by CVB3 infection

Ectopic calcification was detected in the heart, pancreas, and lung (Fig. 2A). Specifically, calcium deposition was detected in cardiac muscle and pancreatic acinar cells that displayed drastic inflammatory and apoptotic damage. Calcification was also observed in interstitial cells of CVB3-infected lung tissue, although inflammatory and apoptotic damage was not observed following viral infection. However, other tissues such as the spleen, kidney, brain, liver, aorta, skeletal muscle, skin, fat, and testis appeared normal in CVB3-infected mice (Supplementary Fig. 2). Our results indicate that the ectopic calcification apparent in CVB3-infected tissues occurred at sites of inflammatory and apoptotic tissue damage.

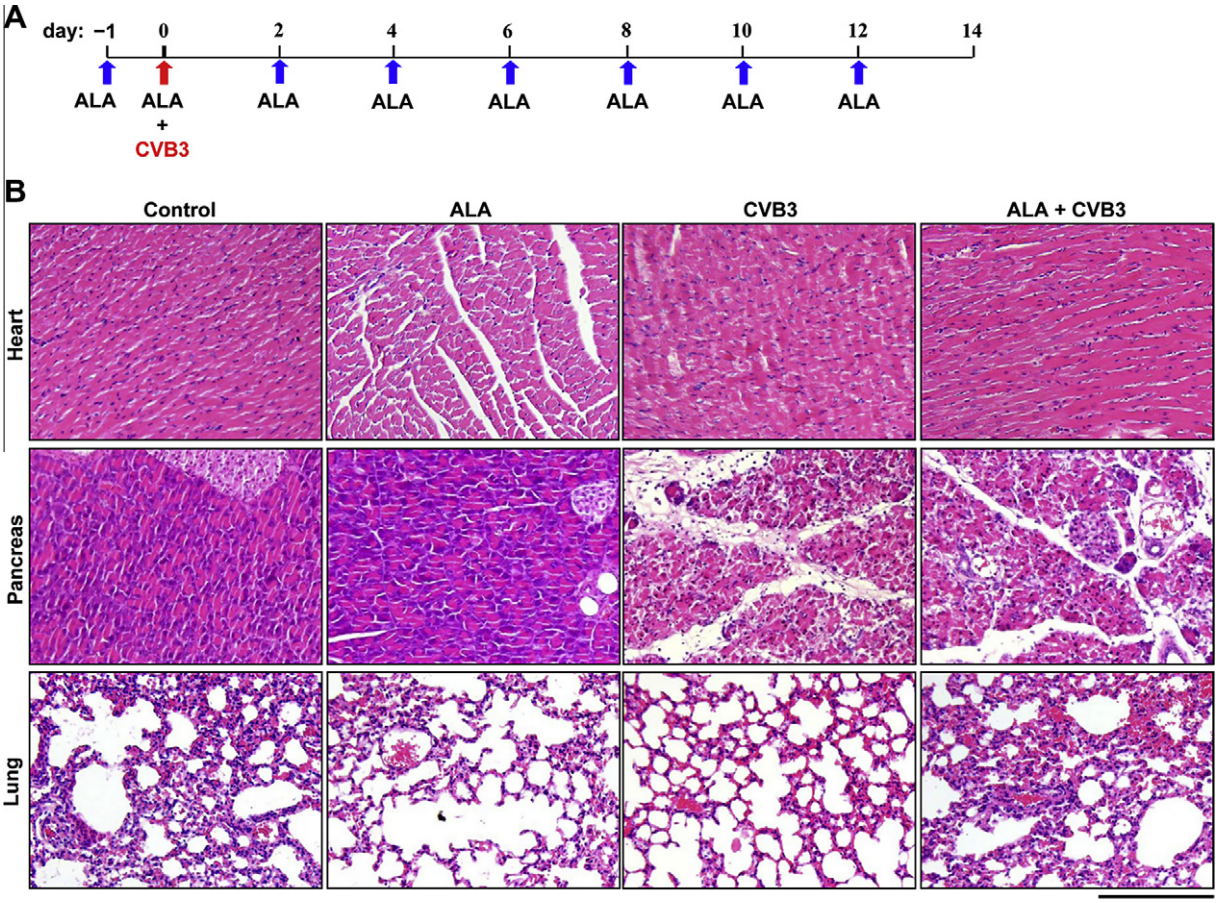

Fig. 3. Histological analysis of CVB3-infected tissues after ALA treatment. (A) Experimental strategy for the treatment of CVB3-infected mice with ALA. After ALA treatment for 1 day, CVB3 and/or ALA was injected at day 0, and ALA was injected every 2 days thereafter. Mice were sacrificed on day 14. (B) Tissue sections from mice treated with control ($n = 7$), ALA ($n = 7$), CVB3 ($n = 7$), or both CVB3 and ALA ($n = 7$) were stained with HE at 14 days post-injection. Representative images are shown. Scale bar, 100 μm.

Ectopic calcification of soft tissues has been reported to be a cell-mediated, active pathological process similar to bone formation or osteogenesis [15]. We next examined the expression levels of several marker genes necessary to osteoblast differentiation in order to investigate the molecular mechanism underlying CVB3-induced ectopic calcification. Quantitative real-time PCR analysis was carried out using specific primers for nine genes involved in osteogenic signaling. As shown in Fig. 2B, six genes, including *BMP2*, *SPARC*, *Runx2*, *OPN*, *Col1α1*, and *Osx*, showed greater than twofold increases in expression in CVB3-infected heart tissue. Expression of three genes (*SPARC*, *OPN*, and *Col1α1*) in the pancreas and two genes (*BMP2* and *Alp*) in the lung was upregulated by more than twofold in CVB3-infected mice compared with control mice. Together, these data suggest that osteogenic genes could play a pivotal role in ectopic calcification following CVB3 infection.

3.3. Effect of α-lipoic acid on CVB3-induced ectopic calcification

We previously reported that ALA inhibits aortic calcification in mice [16]. Therefore, we tested the effect of ALA on CVB3-induced ectopic calcification, as presented in Fig. 3A. Treatment with ALA to CVB3-infected mice restored normal nuclear morphology and cell arrangement in heart tissue and induced mild inflammatory infiltration in interstitial cells in the pancreas, suggesting that ALA could play a role in attenuating inflammatory tissue damage (Fig. 3B). ALA significantly ameliorated CVB3-induced ectopic calcification in the heart, pancreas, and lung, as revealed by calcium content quantification (Fig. 4A). Furthermore, analysis of osteogenic gene expression showed that the expression of three genes (*SPARC*, *OPN*, and *Col1α1*) stimulated by CVB3 infection was downregulated following ALA treatment in virus-infected heart tissue (Fig. 4B). Expression levels of three genes (*SPARC*, *OPN*, and *Col1α1*) in the pancreas and two genes (*BMP2* and *Alp*) in the lung were also reduced by ALA treatment in CVB3-infected mice (Fig. 4B). Together, these results indicate that ALA attenuates CVB3-induced calcification, possibly through the reduction of inflammatory damage and downregulation of osteogenic gene expression.

4. Discussion

In our analysis of the pathological signs of CVB3 infection in a mouse model, CVB3 infection resulted in severe damage to the heart and pancreas compared to other tissues as a result of persistent inflammation, and both body weight and subcutaneous fat content were reduced in CVB3-infected mice due to apparent mal-

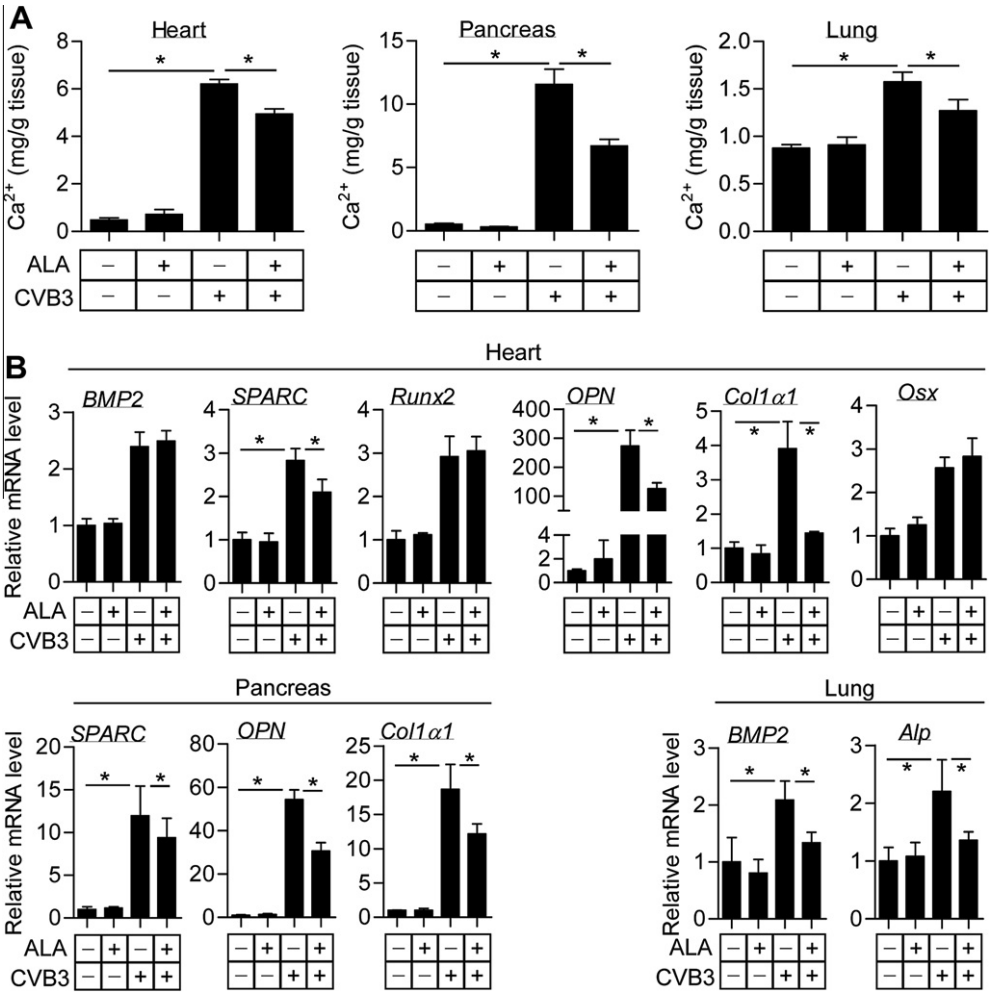

Fig. 4. Effects of ALA on CVB3-induced ectopic calcification and osteogenic gene expression. (A) Quantification of calcium content in mice treated with control ($n = 7$), ALA ($n = 7$), CVB3 ($n = 7$), or both CVB3 and ALA ($n = 7$). Quantitative data are presented as milligrams of calcium per gram of tissue as well as means ± SD. $^*P < 0.01$. (B) Relative gene expression analysis of osteogenic markers in heart, pancreas, and lung tissues from mice treated with control ($n = 5$), ALA ($n = 5$), CVB3 ($n = 5$), or both CVB3 and ALA ($n = 5$). Quantification of mRNA expression is represented as a fold difference relative to control and is normalized to an endogenous control (*β-actin*). Values are expressed as means ± SD. $^*P < 0.01$.

nutrition and subsequent increased consumption of fatty acids to satisfy the energy demands of other tissues.

Pathogenesis of soft tissue calcification is known to involve multiple and complex factors as follows: (i) metabolic factors, including oxidative stress, inorganic phosphate, and vitamin D [8,17,18], (ii) inflammation and inflammatory cytokines [19,20], (iii) apoptosis and apoptotic bodies [7], (iv) activation of osteogenic genes such as *BMP2*, *Runx2*, osterix, collagen type I, alkaline phosphatase, osteopontin, and osteocalcin [8,9], (v) circulating regulators, including fetuin A, matrix Gla protein, osteoprotegerin/RANKL, Klotho, and fibroblast growth factor-23 [10,21–23], and (vi) several clinical factors, including diabetes, chronic kidney disease, and osteoporosis [3,4,24]. In the present study, we observed that CVB3 infection resulted in inflammatory and apoptotic damage to the heart and pancreas. Apoptosis in CVB3-infected tissues is thought to be a direct effect of viral infection, whereas inflammatory cell infiltration is an indirect effect caused by host immune responses. Such damage may be a result of energy depletion in virus-infected cells as well as inflammatory reactions in tissue surrounding the infected lesion. In addition, expression of osteogenesis-associated genes was upregulated in CVB3-infected tissues. For example, six genes (*BMP2*, *SPARC*, *Runx2*, *OPN*, *Col1α1*, and *Osx*) in the heart, three genes (*SPARC*, *OPN*, and *Col1α1*) in the pancreas, and two genes (*BMP2* and *Alp*) in the lung were significantly stimulated by CVB3 infection, a result consistent with previous observations that abnormal soft tissue calcification is closely associated with osteogenic mineralization processes [8,9]. Taken together, our data suggest that pathogenetic factors such as inflammation, apoptosis, and induction of osteogenic genes play essential roles in CVB3-mediated ectopic calcification.

ALA, a naturally occurring antioxidant, is known to be a potent and ideal antioxidant capable of directly scavenging oxidants and enhancing levels of other antioxidants, and it inhibits the intrinsic mitochondrial apoptotic pathway [25,26]. ALA has been shown to be an efficient therapeutic agent for the prevention and treatment of diabetes and cardiovascular disease [27,28]. In addition, our group previously reported that ALA treatment results in the reduction of vascular calcification by inhibiting VSMC apoptosis via restoration of mitochondrial function [16]. Here, we demonstrated that ALA treatment in CVB3-infected mice resulted in decreased virus-induced ectopic calcification via reduction of the inflammatory response, apoptotic tissue damage, and osteogenic signaling. This study further suggests that ALA may be of interest for the treatment of abnormal soft tissue calcification.

Acknowledgments

This work was supported by grants from The National Research Foundation of Korea by the Korean Government (nos. 2010-0012161 and 2012-0000282 to D.J.).

Appendix A. Supplementary data

Supplementary data associated with this article can be found, in the online version, at http://dx.doi.org/10.1016/j.bbrc.2013.01.061.

References

[1] M. Murshed, M.D. McKee, Molecular determinants of extracellular matrix mineralization in bone and blood vessels, Curr. Opin. Nephrol. Hypertens. 19 (2010) 359–365.
[2] E.D. Chan, D.V. Morales, C.H. Welsh, M.T. McDermott, M.I. Schwarz, Calcium deposition with or without bone formation in the lung, Am. J. Respir. Crit. Care Med. 165 (2002) 1654–1669.
[3] G.P. Fadini, M. Albiero, L. Menegazzo, E. Boscaro, S. Vigili de Kreutzenberg, C. Agostini, A. Cabrelle, G. Binotto, M. Rattazzi, E. Bertacco, R. Bertorelle, L. Biasini, M. Mion, M. Plebani, G. Ceolotto, A. Angelini, C. Castellani, M. Menegolo, F. Grego, S. Dimmeler, F. Seeger, A. Zeiher, A. Tiengo, A. Avogaro, Widespread increase in myeloid calcifying cells contributes to ectopic vascular calcification in type 2 diabetes, Circ. Res. 108 (2011) 1112–1121.
[4] M. Schoppet, R.C. Shroff, L.C. Hofbauer, C.M. Shanahan, Exploring the biology of vascular calcification in chronic kidney disease: what's circulating?, Kidney Int 73 (2008) 384–390.
[5] W. Karwowski, B. Naumnik, M. Szczepanski, M. Mysliwiec, The mechanism of vascular calcification-a systematic review, Med. Sci. Monit. 18 (2012) RA1–11.
[6] K. Oka, K. Oohira, Y. Yatabe, T. Tanaka, K. Kurano, R. Kosugi, M. Murata, H. Hakozaki, T. Nishikawa, Y. Tsutsumi, Fulminant myocarditis demonstrating uncommon morphology-a report of two autopsy cases, Virchows Arch. 446 (2005) 259–264.
[7] D. Proudfoot, J.N. Skepper, L. Hegyi, M.R. Bennett, C.M. Shanahan, P.L. Weissberg, Apoptosis regulates human vascular calcification in vitro: evidence for initiation of vascular calcification by apoptotic bodies, Circ. Res. 87 (2000) 1055–1062.
[8] S.A. Steitz, M.Y. Speer, G. Curinga, H.Y. Yang, P. Haynes, R. Aebersold, T. Schinke, G. Karsenty, C.M. Giachelli, Smooth muscle cell phenotypic transition associated with calcification: upregulation of Cbfa1 and downregulation of smooth muscle lineage markers, Circ. Res. 89 (2001) 1147–1154.
[9] Y. Sun, C.H. Byon, K. Yuan, J. Chen, X. Mao, J.M. Heath, A. Javed, K. Zhang, P.G. Anderson, Y. Chen, Smooth muscle cell-specific runx2 deficiency inhibits vascular calcification, Circ. Res. 111 (2012) 543–552.
[10] G. Luo, P. Ducy, M.D. McKee, G.J. Pinero, E. Loyer, R.R. Behringer, G. Karsenty, Spontaneous calcification of arteries and cartilage in mice lacking matrix GLA protein, Nature 386 (1997) 78–81.
[11] E. Neven, P.C. D'Haese, Vascular calcification in chronic renal failure: what have we learned from animal studies?, Circ Res. 108 (2011) 249–264.
[12] J.J. Hsu, Y. Tintut, L.L. Demer, Murine models of atherosclerotic calcification, Curr. Drug Targets 9 (2008) 224–228.
[13] J. Atkinson, Age-related medial elastocalcinosis in arteries: mechanisms, animal models, and physiological consequences, J. Appl. Physiol. 105 (2008) 1643–1651.
[14] K. Lee, H. Kim, H.S. Park, K.-J. Kim, H. Song, H.-I. Shin, H.-S. Kim, D. Seo, H. Kook, J.-H. Ko, D. Jeong, Targeting of the osteoclastogenic RANKL-RANK axis prevents osteoporotic bone loss and soft tissue calcification in coxsackievirus B3-infected mice, J. Immunol. 190 (2013) 1623–1630.
[15] X. Li, H.Y. Yang, C.M. Giachelli, Role of the sodium-dependent phosphate cotransporter, Pit-1, in vascular smooth muscle cell calcification, Circ. Res. 98 (2006) 905–912.
[16] H. Kim, H.J. Kim, K. Lee, J.M. Kim, H.S. Kim, J.R. Kim, C.M. Ha, Y.K. Choi, S.J. Lee, J.Y. Kim, R.A. Harris, D. Jeong, I.K. Lee, Alpha-lipoic acid attenuates vascular calcification via reversal of mitochondrial function and restoration of Gas6/Axl/Akt survival pathway, J. Cell. Mol. Med. 16 (2012) 273–286.
[17] C.H. Byon, A. Javed, Q. Dai, J.C. Kappes, T.L. Clemens, V.M. Darley-Usmar, J.M. McDonald, Y. Chen, Oxidative stress induces vascular calcification through modulation of the osteogenic transcription factor Runx2 by AKT signaling, J. Biol. Chem. 283 (2008) 15319–15327.
[18] J.J. Hsu, Y. Tintut, L.L. Demer, Vitamin D and osteogenic differentiation in the arterywall, Clin. J. Am. Soc. Nephrol. 3 (2008) 1542–1547.
[19] Y. Tintut, J. Patel, F. Parhami, L.L. Demer, Tumor necrosis factor-alpha promotes in vitro calcification of vascular cells via the cAMP pathway, Circulation 102 (2000) 2636–2642.
[20] J.S. Shao, S.L. Cheng, J. Sadhu, D.A. Towler, Inflammation and the osteogenic regulation of vascular calcification: a review and perspective, Hypertension 55 (2010) 579–592.
[21] W.L. Lau, E.M. Leaf, M.C. Hu, M.M. Takeno, O.M. Kuro, O.W. Moe, C.M. Giachelli, Vitamin D receptor agonists increase klotho and osteopontin while decreasing aortic calcification in mice with chronic kidney disease fed a high phosphate diet, Kidney Int. 82 (2012) 1261–1270.
[22] P.A. Price, H.H. June, J.R. Buckley, M.K. Williamson, Osteoprotegerin inhibits artery calcification induced by warfarin and by vitamin D, Arterioscler., Thromb., Vasc. Biol. 21 (2001) 1610–1616.
[23] A. Heiss, T. Eckert, A. Aretz, W. Richtering, W. van Dorp, C. Schafer, W. Jahnen-Dechent, Hierarchical role of fetuin-A and acidic serum proteins in the formation and stabilization of calcium phosphate particles, J. Biol. Chem. 283 (2008) 14815–14825.
[24] L.C. Hofbauer, C.C. Brueck, C.M. Shanahan, M. Schoppet, H. Dobnig, Vascular calcification and osteoporosis-from clinical observation towards molecular understanding, Osteoporos. Int. 18 (2007) 251–259.
[25] T.M. Hagen, J. Liu, J. Lykkesfeldt, C.M. Wehr, R.T. Ingersoll, V. Vinarsky, J.C. Bartholomew, B.N. Ames, Feeding acetyl-L-carnitine and lipoic acid to old rats significantly improves metabolic function while decreasing oxidative stress, Proc. Natl. Acad. Sci. USA 99 (2002) 1870–1875.
[26] K.P. Shay, R.F. Moreau, E.J. Smith, A.R. Smith, T.M. Hagen, Alpha-lipoic acid as a dietary supplement: molecular mechanisms and therapeutic potential, Biochim. Biophys. Acta 1790 (2009) 1149–1160.
[27] S. Ghibu, C. Richard, C. Vergely, M. Zeller, Y. Cottin, L. Rochette, Antioxidant properties of an endogenous thiol: alpha-lipoic acid, useful in the prevention of cardiovascular diseases, J. Cardiovasc.Pharmacol. 54 (2009) 391–398.
[28] A.R. Smith, S.V. Shenvi, M. Widlansky, J.H. Suh, T.M. Hagen, Lipoic acid as a potential therapy for chronic diseases associated with oxidative stress, Curr. Med. Chem. 11 (2004) 1135–1146.